https://doi.org/10.5194/gchron-2021-29
Preprint. Discussion started: 25 October 2021

Short communication: Modelling competing effects of cooling rate, grain size and radiation damage in low temperature thermochronometers

David M. Whipp[1]★, Dawn A. Kellett[2]★, Isabelle Coutand[3]

[1]Department of Geosciences and Geography, University of Helsinki, FI-00014 University of Helsinki, Finland, ORCiD ID: 0000-0002-3820-6886
[2]Geological Survey of Canada - Atlantic, Natural Resources Canada, Dartmouth, B2Y 4A2, Canada, ORCiD ID: 0000-0002-4558-4703
[3]Department of Earth and Environmental Sciences, Dalhousie University, Halifax, B3H 4R2, Canada, ORCiD ID:

Correspondence to: Dawn A. Kellett (dawn.kellett@canada.ca)

★ These authors contributed equally to this work.

Abstract. Low temperature multi-thermochronometry, in which the (U-Th)/He and fission track methods are applied to minerals such as zircon and apatite, is a valuable approach for documenting rock cooling histories and relating them to geological processes. Here we explore the behaviours of two of the most commonly applied low temperature thermochronometers, (U-Th)/He in zircon (ZHe) and apatite (AHe), and directly compare against the apatite fission track (AFT) thermochronometer for different forward-modelled cooling scenarios. We consider the impacts that common variations in effective spherical radius (ESR) and effective Uranium concentration (eU) may have on cooling ages and closure temperatures under a range of different cooling rates. This exercise highlights different scenarios under which typical age relationships between these thermochronometers (ZHe > AFT > AHe) are expected to collapse, or partially to fully invert. We anticipate that these predictions and the associated software we provide will be a useful tool for teaching, planning low temperature multi-thermochronometry studies, and for continued exploration of the relative behaviours of these thermochronometers in the temperature-time space through forward models.

1 Introduction

Low temperature multi-thermochronometry, particularly involving the incorporation of both (U-Th)/He and fission track datasets, represents the state of the art for developing temperature-time (T-t) evolutions for rocks in the upper continental crust. Track length distributions in fission track thermochronology and effective Uranium (eU; calculated as [U]+0.235[Th])-age relationships in (U-Th)/He thermochronology together have the potential to provide highly detailed rock T-t histories that can be used to interpret and reconstruct a diverse range of geological processes and their rates, from long-term

https://doi.org/10.5194/gchron-2021-29
Preprint. Discussion started: 25 October 2021

landscape evolution of Precambrian shields (e.g. Lorencak et al., 2004; Danišík et al., 2008) to rifting (e.g. Cogné et al., 2011; Ricketts et al., 2016) to orogenic construction and collapse (e.g. Thomson and Ring, 2006; Coutand et al., 2014; Toraman et al., 2014). The diffusion/annealing models for these thermochronometric systems, especially for the common accessory minerals zircon and apatite, are fairly well accepted across the scientific community, and embedded into widely-used thermal modeling softwares such as *HeFTy* (Ketcham, 2005) and *QTQt* (Gallagher, 2012), as well as thermokinematic models such as *Pecube* (Braun, 2003). While it has become common practice to input measured (U-Th)/He and fission track data into thermal modelling software to invert for best-fit thermal histories, this type of application and interpretative products can obscure visualization of the complex relationships that exist between internal (e.g., eU, grain size, mineral chemistry) and external (thermodynamical effects of the various and competing geological processes that lead to changes in rock T) parameters (or factors) controlling measured thermochronometric ages. Classical plots of closure temperature vs. cooling rate, in which the relationships for mineral-specific thermochronometers form a stack of near-parallel curves (e.g., Fig. 1 of Reiners and Brandon, 2006), are widely cited in courses and the literature, and often form the starting point for discussing the significance of low temperature thermochronological datasets. However, those plots seldom include the age and closure temperature effects in broadly accepted He diffusion models that incorporate crystal damage and annealing (Flowers et al., 2009; Guenthner et al., 2013; Guenthner 2021). Forward modelling tools (including *HeFTy* and *QTQt*) are well-suited for exploring parameters such as grain size and eU, because additional complicating factors that apply to empirical datasets, such as chemical zoning or unexplained age dispersion, can be ignored, and because thermal histories are user-defined rather than non-unique unknowns. However, batch-processing hundreds to thousands of forward models to evaluate how broad ranges of input parameters affect predicted ages or closure temperatures can be tedious. Here, we have designed a simple forward model software to examine differences in predicted thermochronometer ages and closure temperatures with a particular focus on comparing (U-Th)/He zircon and apatite systems (hereafter ZHe and AHe, respectively) to the apatite fission track (AFT) system. Our goal is to explore and compare the range of behaviours of these different systems that could be expected for different grain sizes and eU conentrations by generating thermochronometric datasets for a wide range of linear cooling rates. The plots and associated code we provide are useful interpretive tools for designing multi-thermochronometric studies, and for conceptualizing expected thermochronometer behaviours under various geological conditions.

2 Predicting thermochronometer ages and closure temperatures

We used existing thermochronometer age prediction algorithms to predict AHe, AFT, and ZHe thermochronometer ages and effective closure temperatures for a range of cooling rates, eU concentrations, and grain radii. Rather than calculating thermal histories using a heat transfer model, we generated synthetic linear cooling histories with cooling from 250 to 0 °C at constant rates of 0.1 - 100 °C/Myr (Figure 1). This approach allows exploration of the effects of a wide range of plausible cooling rates through the partial retention and partial annealing zones of all three thermochronometers. To explore the effects of radiation damage on He diffusion, we considered ranges in eU concentration of 1

– 150 ppm for AHe and 1 – 4000 ppm for the ZHe system. These different ranges are intended to reflect typical eU values for natural apatite and zircon grains that could be the target for dating (e.g., Donelick et al., 2005; Cherniak and Watson, 2003). Finally, we varied effective spherical radius (ESR) from 40 – 100 μm for both zircon and apatite, as an estimate of the natural variation in ESR in dated minerals.

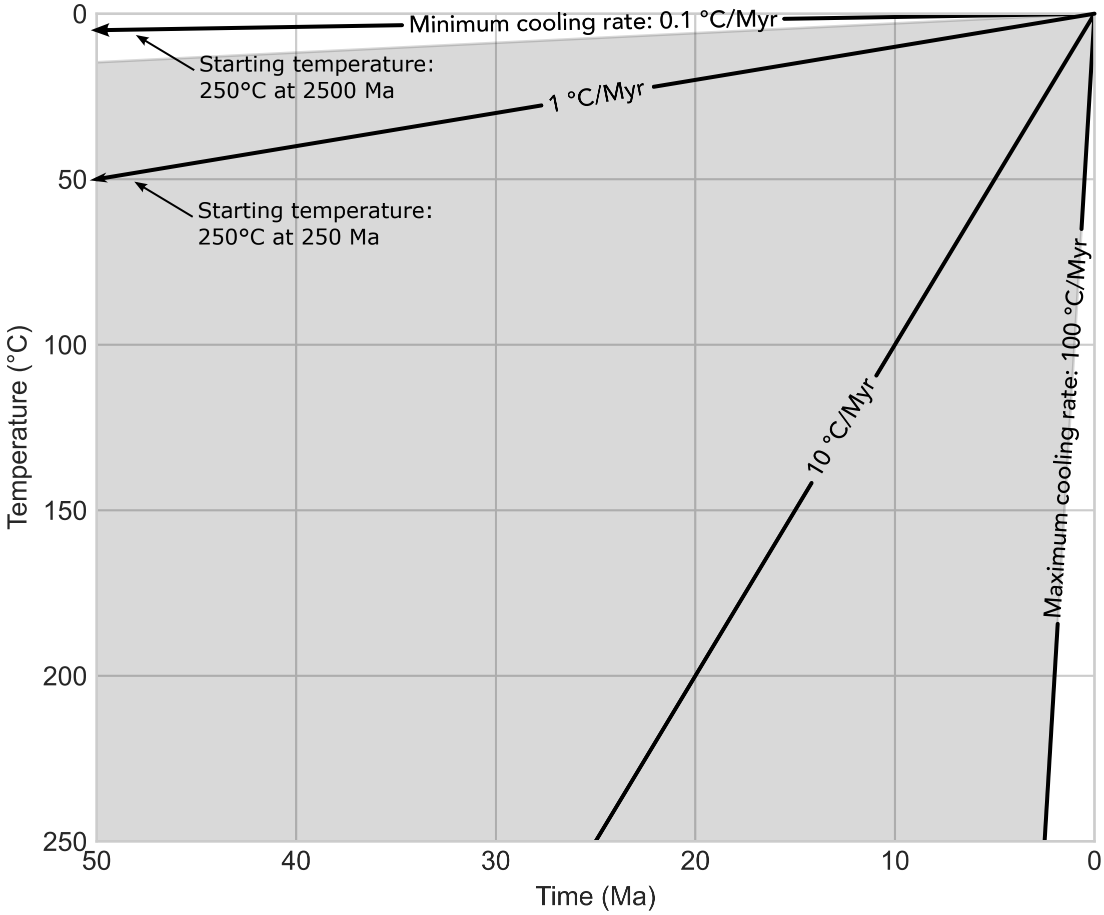

Figure 1: Temperature-time plot showing the range of cooling histories (grey shaded area) used for thermochronometer age prediction. All scenarios start at 250 °C and cool to 0 °C at a constant rate. Note that the x-axis of the plot is truncated for readability. Fig. 2 shows results for a 10 °C/Myr cooling history, while Figs. 3 and 4 show results for the full shaded region in log space.

Using the predefined ranges in cooling rate, eU concentration, and ESR as inputs, we calculated thermochronometer ages and effective closure temperatures using the fission track annealing model of Ketcham et al. (2007) for AFT ages, and the radiation damage accumulation and annealing models of Flowers et al. (2009) and Guenthner et al. (2013) for simulating the effects of radiation damage on the predicted AHe and ZHe ages, respectively. For all cases, the effective closure temperature was estimated by reporting the temperature in the cooling history at the time of the predicted thermochronometer age.

The software used for thermochronometer age and closure temperature prediction is available as supplementary material to this article. Using this software it is possible for users to reproduce and customize versions of Figures 2-4. Furthermore, in addition to the linear cooling histories presented here it is possible to define more complex thermal histories involving multi-stage cooling and reheating events, as well as export predicted AFT length distributions.

3 Exploring the multi-thermochronometry space

3.1 Contrasting He behaviour in apatite and zircon under cooling scenarios

He is produced in apatite and zircon primarily via alpha decay of U and Th, and its mobility (loss/retention) in apatite and zircon forms the basis for AHe and ZHe thermochronometers, which are broadly applied by the Earth Sciences research community to determine temperature-time (T-t) points or paths for analysed rock samples. He mobility is a thermally-controlled volume diffusion process and therefore sensitive to grain size (e.g., Reiners and Farley, 2001), which is typically quantified as ESR (Wolf et al., 1996). However, He diffusion behaviour in both apatite and zircon is also dependent on the progressive accumulation of internal crystal damage caused by alpha decay. Crystal damage occurs at a rate determined by the eU concentration in a crystal, and is thought to anneal in a similar way, and under somewhat similar thermal conditions to those needed for annealing of fission tracks (Flowers et al., 2009; Guenthner et al., 2013; Guenthner, 2021). Consequently, both the pre-He retention thermal history and the chemistry of dated crystals (which together determine how much crystal damage has accumulated) are essential inputs for modelling He diffusional behaviour and determining grain specific AHe and ZHe closure temperatures. He diffusivity in apatite has been found to generally decrease with greater accumulated alpha damage, such that more damaged grains are more retentive and have higher AHe closure temperatures (Shuster 2006; Shuster et al., 2009). Zircon commonly incorporates significantly more U (and hence eU) into its structure compared to apatite, with eU concentrations of 100-1000 ppm being typical and eU >4000 ppm being not uncommon (compared to more typical eU concentrations of 1-100 ppm in apatite). Zircon is also more resistant to geological cycling than apatite. Thus, the potential for accumulating radiation damage is much higher in zircon compared to apatite. At low to intermediate levels of alpha decay-induced crystal damage, He diffusivity in zircon decreases with greater accumulated alpha damage, but at high levels of damage, He diffusivity increases significantly (Guenthner et al., 2013). Consequently, possible closure temperatures for the ZHe system show a much larger range than for AHe (e.g., Ault et al., 2019). Finally, we note that since annealing of fission tracks in apatite is not subject to volume diffusion, AFT ages are not influenced by either apatite grain size or eU concentration (e.g. Kohn et al., 2009).

First, we investigated the extent of grain size and eU concentration controls on He diffusion (and resulting (U-Th)/He closure temperatures) in zircon and apatite for a constant cooling rate of 10 °C/Myr and typical ESR ranges (40-100 µm) and eU concentrations (1-150 ppm for apatite, and 1-4000 ppm for zircon; Fig. 2). This cooling history results in a total model run time of 25 Myr. At this cooling rate and timescale, the AHe (Fig. 2a,b) and ZHe (Fig. 2c,d) thermochronometers show contrasting relationships. AHe cooling ages are strongly positively correlated with ESR, with smaller grains having younger cooling ages and lower closure temperatures, and larger grains having older cooling ages and higher closure temperatures (Fig. 2a, b). The AHe cooling ages are much less sensitive to variations in eU concentration, although still positively correlated. These plots show that, over this relatively short timescale, alpha damage exerts little influence on He diffusion (or diffusional behaviour) in apatite, and AHe closure temperature varies by less than 15 °C across these scenarios. However, ZHe cooling ages show the opposite relationship (Fig. 2c, d). The higher natural range in zircon eU concentrations, and the resultant damage to the zircon crystal from those higher dosages of alpha decay, controls the diffusion behaviour of He in zircon even in this relatively rapid cooling scenario. Consequently, for the same cooling history as that modelled for apatite, ZHe cooling ages and closure temperatures are strongly positively correlated with eU concentration, relatively insensitive to ESR, and ZHe closure temperature varies >100 °C.

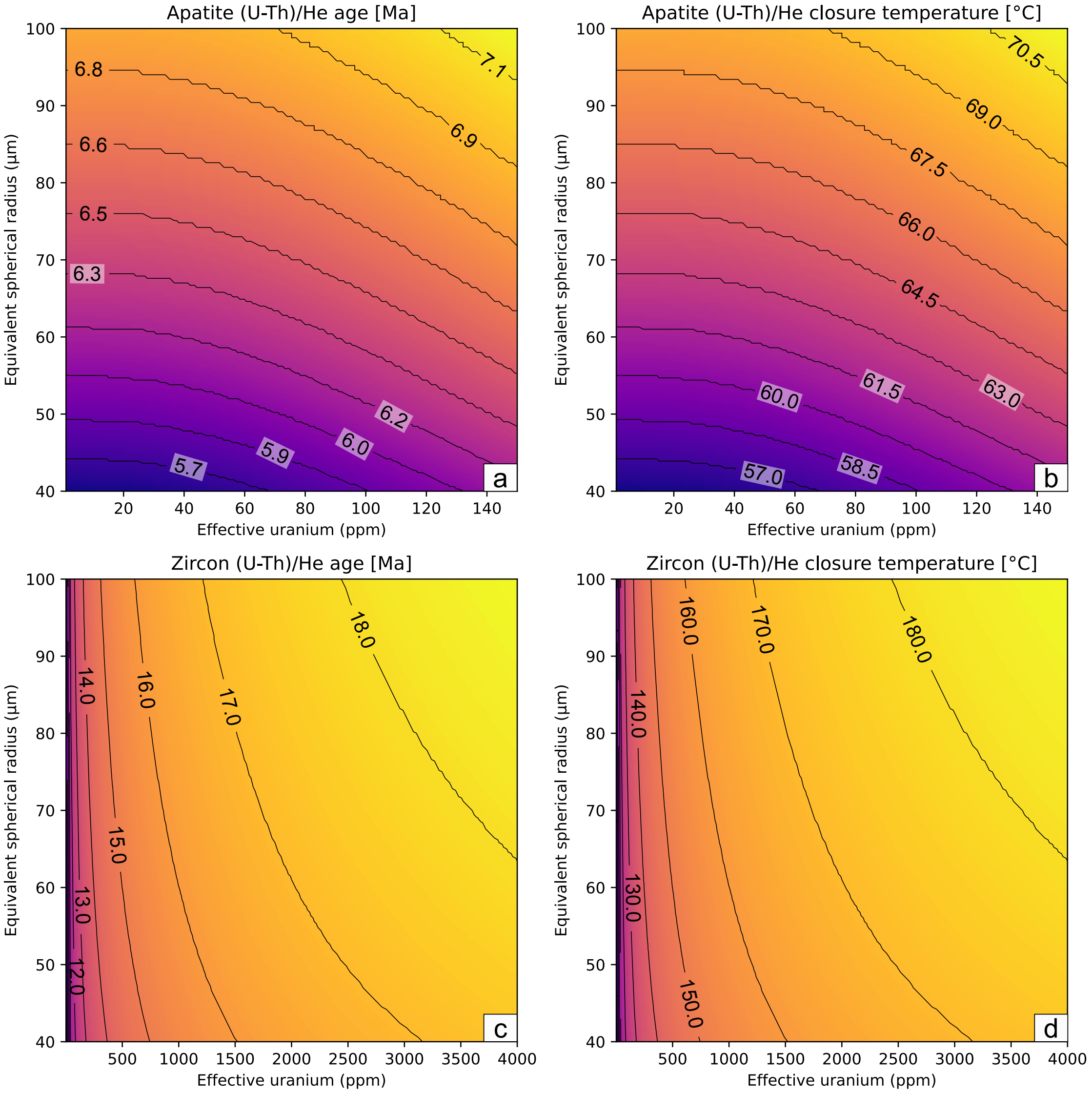

Figure 2: Contoured model (U-Th)/He cooling ages (a) and closure temperatures (b) for apatite, and model (U-Th)/He cooling ages (c) and closure temperatures (d) for zircon of different effective spherical radii and eU concentrations (ppm). All panels are calculated for cooling from 250 °C to 0 °C at a constant rate of 10 °C/Myr. The plots comprise predicted ages and closure temperatures for 10,201 forward models.

In contrast to Figure 2, where only a single cooling rate was used, we next explore the influence of the intra-grain parameters (grain size, eU) on closure temperature for a wide range of geologically plausible cooling rates (0.1-100 °C/Myr; Fig. 3). We first fixed the eU at "typical" values of 10 ppm for apatite and 100 ppm for zircon while varying ESR (Fig. 3a, c), and then fixed ESR at "typical" values of 45 μm for apatite and 60 μm for zircon while varying eU (Fig. 3b, d). In this parameter space, closure temperatures for AHe range from ~40-85 °C, closure temperatures for ZHe vary from ~0-180 °C, and closure temperature relationships for AHe and ZHe are again strongly contrasting. For eU of 10 ppm,

https://doi.org/10.5194/gchron-2021-29
Preprint. Discussion started: 25 October 2021

AHe closure temperature is negatively correlated with cooling rate at slow cooling rates, but undergoes an inflection at ~0.5-1 °C/Myr beyond which closure temperatures are positively correlated with cooling rate at faster cooling rates, with variations in ESR maintaining an overall positive correlation with closure temperature for all cooling rates (Fig. 3a). For eU of 100 ppm, ZHe closure temperatures, in contrast, are negatively correlated with cooling rate, with a subtle inflection inverting this relationship at very slow cooling rates approaching 0.1 °C/Myr. As for apatite, zircon ESR variations show a positive correlation with closure temperature under the full range of cooling rates (Fig. 3c).

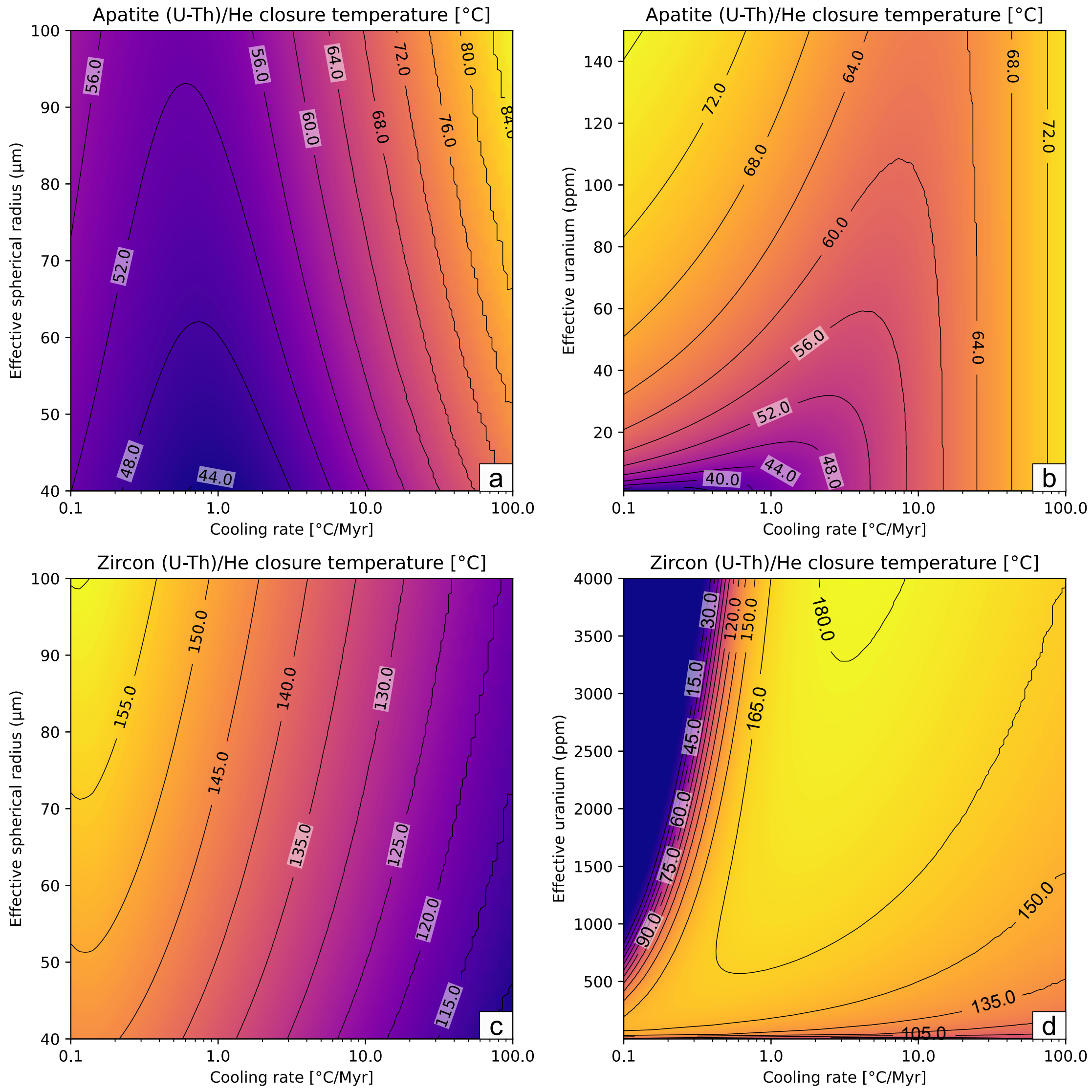

Figure 3: Contoured closure temperatures for the apatite and zircon (U-Th)/He systems as functions of cooling rate, effective spherical radius, and eU concentration. (a) Apatite: eU is fixed at 10 ppm; (b) apatite: ESR is fixed at 45 µm; (c) zircon: eU is fixed at 100 ppm; (d) zircon: ESR is fixed at 60 µm The plots comprise predicted closure temperatures for 20,402 forward models and each model applies a constant cooling rate between 0.1-100 °C/Myr.

https://doi.org/10.5194/gchron-2021-29
Preprint. Discussion started: 25 October 2021

For a fixed ESR of 45 μm, the AHe system shows closure temperatures that are positively correlated with eU and negatively correlated with cooling rate at slow cooling rates, but undergoes an inflection between 1-10 °C/Myr beyond which closure temperatures are positively correlated with cooling rate, and insensitive to eU (Fig. 3b). For the same cooling rate range, a fixed ESR of 60 μm, and range of zircon eU values of 1-4000 ppm, the ZHe system shows closure temperatures that are strongly positively correlated to cooling rate, and strongly negatively correlated to eU concentration for slow cooling rates (≤1 °C/Myr), except for low eU (<50 ppm), such that the closure temperature approaches 0 °C over a significant area of the plot space in which damage accumulation is high (high eU, slow cooling rate; Fig. 3d). This system also shows an inflection, in the vicinity of 0.1-2 °C/Myr, beyond which ZHe closure temperatures are weakly positively correlated to eU, and actually negatively correlated with cooling rate. In other words, fast cooling rates are expected to produce lower ZHe closure temperatures than intermediate cooling rates. Comparison of these four plots (Fig. 3) indicates that ZHe and AHe closure temperatures are not only expected to vary significantly under different cooling rate scenarios, but also that they do not track together, meaning that some conditions simultaneously favour higher AHe and lower ZHe closure temperatures and vice versa. We explore this outcome in more detail in the following section. Differences in closure temperature behaviour should also, of course, be expected for zircon among neighbour samples with different average eU concentration, not to mention within samples for which individual grains show large differences in eU, as is common in detrital samples. Likewise for intra-sample ranges in ESR for apatite or zircon, although these differences are likely more subtle.

3.2 The multi-thermochronometry space of ZHe, AFT and AHe

The relationships between ZHe, AFT and AHe have commonly been summarized as stacked parallel curves in a plot of closure temperature vs. cooling rate (e.g., Reiners and Brandon, 2006), or as having progressively lower closure T ranges in lists of widely applied thermochronometers. However, it is apparent in the above plots that ‘typical’ zircon and apatite are expected to have contrasting He diffusion behaviours under different cooling scenarios. In Figure 4, we provide a visualization of how these different behaviours at high vs. low cooling rate are expected to produce contrasting cooling age and closure temperature relationships among the ZHe, AFT and AHe thermochronometers. In each plot pair, we have predicted ages and closure temperatures of the three thermochronometers for constant cooling rates of 0.1-100 °C/Myr, corresponding to cooling from 250 °C in 2500 to 2.5 Myr, respectively (Figs. 1, 4). For simplicity, we varied eU in the stacked plots from low (apatite = 1.0 ppm; zircon = 10 ppm), to intermediate (apatite = 10 ppm; zircon = 100 ppm), to high (apatite = 200 ppm; zircon = 1000 ppm) eU concentrations. We note that in nature, a rock with high eU zircon may not necessarily have high eU apatite, and vice versa, but present the plots in this way for simplicity. In all plots, AFT is unaffected by eU, and shows near-linear relationships between predicted age and cooling rate, and closure temperature and cooling rate in log-log and semi-log space, respectively. To estimate the conditions in which measured ages may differ between systems including their measurement uncertainties, we have predicted cooling ages as age swaths with "typical” uncertainties of 10% for AHe and ZHe, and 20% for AFT.

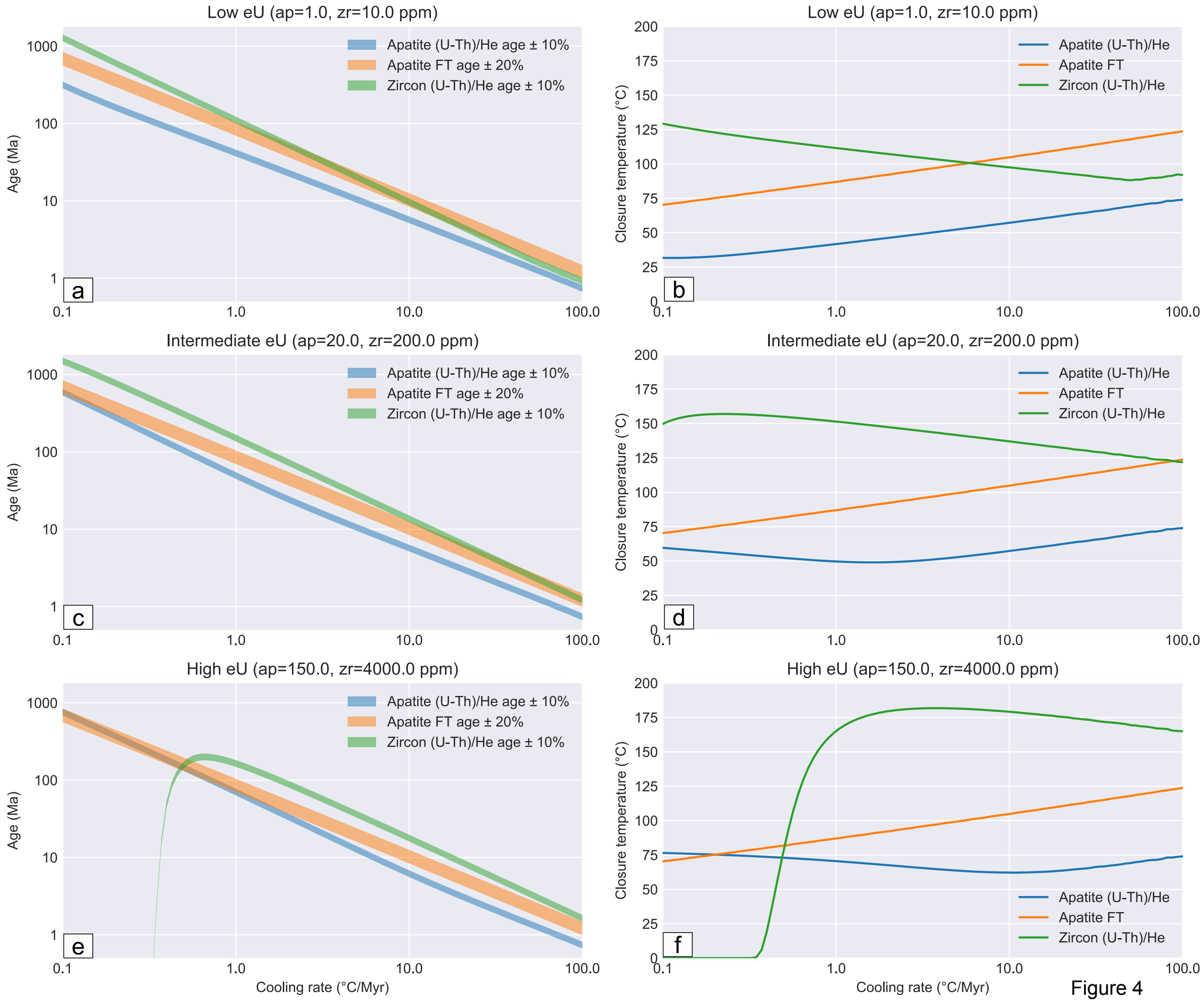

Figure 4

Figure 4: Predicted thermochronometer ages (left) and closure/annealing temperatures (right) for low (top), intermediate (middle), and high (bottom) eU concentrations, as a function of cooling rate. The plots comprise predicted ages and closure temperatures for 303 forward models and each model applies a constant cooling rates between 0.1-100 °C/Myr. The coloured swaths for the predicted ages (a, c, e) indicate the mean age plus or minus the indicated percent uncertainty.

The AHe cooling ages and closure temperatures are non-linear in this parameter space (Fig. 4), being uniformly younger/lower than AFT, except for high eU apatite at very slow cooling rates (Fig. 4e, f), for which AHe cooling ages and closure temperatures could be slightly older and higher than AFT. The lowest AHe closure temperatures are expected for slow cooling rates of 0.1-2 °C/myr and low-intermediate eU (Fig. 4b, d), while at high eU, the lowest AHe closure temperatures are expected for intermediate-fast cooling rates of 10-20 °C/Myr (Fig. 4f). ZHe cooling ages and closure temperatures are also generally non-linear. At slower cooling rates (<10 °C/Myr for low eU; <50 °C/Myr for intermediate eU), ZHe cooling ages and closure temperatures are expected to be older/higher than AFT, while at faster cooling rates (>10 °C/Myr for low eU; >50 °C/Myr for intermediate eU), they are younger/lower than AFT (Fig. 4a-d). The high eU scenario clearly shows the remarkable changes in He diffusivity for high alpha dosages in zircon, with a dramatic drop in cooling age and closure temperature expected for cooling rates slower than ~1 °C/Myr. Thus, although under most of the parameter space explored, cooling ages are expected to progressively decrease from ZHe to AFT to AHe, there are conditions under which this relationship partially (AFT>ZHe for fast cooling rates, low/intermediate zircon eU) or fully (AHe>AFT>ZHe for very slow cooling rates and high eU) inverts, even when including large error bars for the calculated ages. These relationships may in part explain observations from empirical studies. For example, AHe > AFT ages have been commonly reported from geologically old (cratonic) regions (e.g., Hansen and Reiners, 2006; Danišík et al., 2008; Flowers and Kelley, 2011). As shown in these plots, AHe and AFT ages are expected to converge and invert for high eU in apatite and timescales >250 Ma (Fig. 4f). AHe > ZHe ages have also been reported from cratonic samples with high-damage zircon (Johnson et al, 2017). The highest damage zircon simulated in the linear cooling scenarios presented here is represented by slow cooling of high eU zircon (Fig. 4e, f). These plots form a first-order guide to investigating the character of regional multi-thermochronometry datasets, and the software we provide can be used by the reader to further explore expected relationships and time lags between the chronometers under either constant, or multi-stage linear cooling and heating scenarios, as well as other parameters such as apatite Cl content in the context of the AFT system.

4 Summary

The ZHe, AFT and AHe methods are commonly used together in samples to develop low temperature thermal histories for rocks and regions. In this short communication, we have explored the range of cooling age and corresponding closure temperature responses expected for ZHe and AHe, relative to the AFT thermochronometry system, by exploring typical parameter ranges for these systems using simple forward temperature-time models. We compared the relative effects of grain size and eU on ZHe and AHe closure temperature and cooling age, and showed that under typical mineral-specific ranges of eU, the ZHe system is highly sensitive to eU and comparatively insensitive to grain size, while the AHe system is sensitive to grain size and less sensitive to eU. The complex relationships that the ZHe and AHe systems exhibit with respect to eU and grain size result in contrasting relationships among the three thermochronometers under different linear cooling scenarios, including convergence between the thermochronometers, and even partial to full inversion of the typical ZHe > AFT > AHe age relationship. The software available from this study provides a new tool to easily forward model multi-thermochronometry relationships, and complements the range of existing modelling software packages for thermochronological research.

Code availability

Software used to produce the figures in this manuscript is available at https://doi.org/10.23729/474ade1f-6f51-40cb-a11c-06ea0f7bfd3c.

Author contribution

All authors conceptualized this study. Whipp wrote the plotting scripts and produced the figures in consultation with Kellett and Coutand. Kellett and Whipp wrote the manuscript. Whipp, Kellett and Coutand developed the discussion, and revised the manuscript.

Acknowledgements

We would like to acknowledge Richard Ketcham for sharing the thermochronometer age prediction algorithms used in *HeFTy*.

References

Ault, A.K., Gautheron, C. and King, G.E., Innovations in (U–Th)/He, fission track, and trapped charge thermochronometry with applications to earthquakes, weathering, surface-mantle connections, and the growth and decay of mountains, Tectonics, 38(11), p.3705-3739, doi:10.1029/2018TC005312, 2019.
Braun, J.: Pecube: A new finite-element code to solve the 3D heat transport equation including the effects of a time-varying, finite amplitude surface topography, Computers & Geosciences, 29, doi:10.1016/S0098-3004(03)00052-9, 787-794, 2003.
Cherniak, D.J. and Watson, E.B., Diffusion in zircon. Reviews in Mineralogy and Geochemistry, 53(1), 113-143, https://doi.org/10.2113/0530113, 2003.
Cogné, N., Gallagher, K. and Cobbold, P.R.: Post-rift reactivation of the onshore margin of southeast Brazil: Evidence from apatite (U–Th)/He and fission-track data, EPSL, 309, 118-130, doi:10.1016/j.epsl.2011.06.025, 2011.
Coutand, I., Whipp Jr, D.M., Grujic, D., Bernet, M., Fellin, M.G., Bookhagen, B., Landry, K.R., Ghalley, S.K. and Duncan, C.: Geometry and kinematics of the Main Himalayan Thrust and Neogene crustal exhumation in the Bhutanese Himalaya derived from inversion of multithermochronologic data. JGR: Solid Earth, 119, 1446-1481, doi:10.1002/2013JB010891, 2014.
Danišík, M., Sachsenhofer, R.F., Privalov, V.A., Panova, E.A., Frisch, W. and Spiegel, C.: Low-temperature thermal evolution of the Azov Massif (Ukrainian Shield–Ukraine)—Implications for interpreting (U–Th)/He and fission track ages from cratons, Tectonophys., 456, 171-179, doi:10.1016/j.tecto.2008.04.022, 2008.
Donelick, R.A., O'Sullivan, P.B. and Ketcham, R.A., 3. Apatite Fission-Track Analysis. Low-Temperature Thermochronology, Reviews in Mineralogy and Geochemistry, 58, 49-94, doi:10.1515/9781501509575-005, 2005.
Flowers, R.M. and Kelley, S.A.: Interpreting data dispersion and "inverted" dates in apatite (U–Th)/He and fission-track datasets: an example from the US midcontinent, Geochimica et Cosmochimica Acta, 75(18), 5169-5186, doi:10.1016/j.gca.2011.06.016, 2011.
Flowers, R.M., Ketcham, R.A., Shuster, D.L. and Farley, K.A.: Apatite (U–Th)/He thermochronometry using a radiation damage accumulation and annealing model. Geoch. Cosmoch. Acta, 73, 2347-2365, doi:10.1016/j.gca.2009.01.015, 2009.

Gallagher, K.: Transdimensional inverse thermal history modeling for quantitative thermochronology, JGR: Solid Earth, 117, doi:10.1029/2011JB008825, 2012.

Guenthner, W.R., Reiners, P.W., Ketcham, R.A., Nasdala, L. and Giester, G.: Helium diffusion in natural zircon: Radiation damage, anisotropy, and the interpretation of zircon (U-Th)/He thermochronology, Am. J. Sci., 313, 145-198, doi:10.2475/03.2013.01, 2013.

Guenthner, W.R.: Implementation of an alpha damage annealing model for zircon (U-Th)/He thermochronology with comparison to a zircon fission track annealing model, G3, 22, doi:10.1029/2019GC008757, 2021.

Hansen, K. and Reiners, P.W.: Low temperature thermochronology of the southern East Greenland continental margin: evidence from apatite (U–Th)/He and fission track analysis and implications for intermethod calibration, Lithos, 92(1-2), 117-136, doi:10.1016/j.lithos.2006.03.039, 2006.

Johnson, J.E., Flowers, R.M., Baird, G.B. and Mahan, K.H.: “Inverted” zircon and apatite (U–Th)/He dates from the Front Range, Colorado: high-damage zircon as a low-temperature (< 50° C) thermochronometer, Earth and Planetary Science Letters, 466, p.80-90, doi:10.1016/j.epsl.2017.03.002, 2017.

Ketcham, R.A.: Forward and inverse modeling of low-temperature thermochronometry data, Rev. Min. Geochem., 58, 275-314, doi:10.2138/rmg.2005.58.11, 2005.

Ketcham, R.A., Carter, A., Donelick, R.A., Barbarand, J. and Hurford, A.J.: Improved modeling of fission-track annealing in apatite, Am. Min., 92, 799-810, doi:10.2138/am.2007.2281, 2007.

Kohn, B.P., Lorencak, M., Gleadow, A.J., Kohlmann, F., Raza, A., Osadetz, K.G. and Sorjonen-Ward, P.: A reappraisal of low-temperature thermochronology of the eastern Fennoscandia Shield and radiation-enhanced apatite fission-track annealing, Geological Society, London, Special Publications, 324(1), 193-216, doi:10.1144/SP324.15, 2009.

Lorencak, M., Kohn, B.P., Osadetz, K.G. and Gleadow, A.J.W.: Combined apatite fission track and (U–Th)/He thermochronometry in a slowly cooled terrane: results from a 3440-m-deep drill hole in the southern Canadian Shield, EPSL, 227, 87-104, doi:10.1016/j.epsl.2004.08.015, 2004.

Ricketts, J.W., Kelley, S.A., Karlstrom, K.E., Schmandt, B., Donahue, M.S. and van Wijk, J.: Synchronous opening of the Rio Grande rift along its entire length at 25–10 Ma supported by apatite (U-Th)/He and fission-track thermochronology, and evaluation of possible driving mechanisms, GSA Bull., 128, 397-424, doi:10.1130/B31223.1, 2016.

Reiners, P.W. and Farley, K.A.: Influence of crystal size on apatite (U–Th)/He thermochronology: an example from the Bighorn Mountains, Wyoming, Earth and Planetary Science Letters, 188(3-4), p.413-420, doi:10.1016/S0012-821X(01)00341-7, 2001.

Reiners, P.W. and Brandon, M.T.: Using thermochronology to understand orogenic erosion. Annu. Rev. Earth Planet. Sci., 34, 419-466, doi:10.1146/annurev.earth.34.031405.125202, 2006.

Shuster, D.L. and Farley, K.A.: The influence of artificial radiation damage and thermal annealing on helium diffusion kinetics in apatite. Geoch. Cosmoch. Acta, 73, 183-196, doi:10.1016/j.gca.2008.10.013, 2009.

Shuster, D.L., Flowers, R.M. and Farley, K.A.: The influence of natural radiation damage on helium diffusion kinetics in apatite, EPSL, 249, 148-161, doi:10.1016/j.epsl.2006.07.028, 2006.

Thomson, S.N. and Ring, U.: Thermochronologic evaluation of postcollision extension in the Anatolide orogen, western Turkey, Tectonics, 25, doi:10.1029/2005TC001833, 2006.

Toraman, E., Teyssier, C., Whitney, D.L., Fayon, A.K., Thomson, S.N. and Reiners, P.W.: Low-temperature thermochronologic record of Eocene migmatite dome emplacement and late Cenozoic landscape development, Shuswap core complex, British Columbia, Tectonics, 33, 1616-1635, doi:10.1002/2013TC003442, 2014.

Wolf, R.A., Farley, K.A. and Silver, L.T.: Helium diffusion and low-temperature thermochronometry of apatite. Geochimica et Cosmochimica Acta, 60(21), p.4231-4240, doi:10.1016/S0016-7037(96)00192-5, 1996.

Assets:
Software used to produce the figures in this manuscript is available at https://doi.org/10.23729/474ade1f-6f51-40cb-a11c-06ea0f7bfd3c.

Short summary:
Multi-thermochronometry, in which methods such as (U-Th)/He dating of zircon and apatite, and apatite fission-track dating are combined, is used to reconstruct rock thermal histories. Our ability to reconstruct thermal histories and interpret the geological significance of measured ages requires modeling. Here we use forward models to explore grain size and chemistry effects on cooling ages and closure temperatures for the (U-Th)/He decay systems in apatite and zircon.